29th EPS Conference on Plasma Phys. and Contr. Fusion Montreux, 17-21 June 2002 ECA Vol. **26B**, P-4.095 (2002)

SEMI-LAGRANGIAN DRIFT-KINETIC CODE FOR SLAB-ITG TURBULENCE

V. Grandgirard, M. Brunetti[1], S. Allfrey[1], A. Bottino[1], P. Bertrand[2], P. Ghendrih, X. Garbet, A. Ghizzo[2],G. Manfredi[1], M.Ottaviani, Y. Sarazin, O. Sauter[1], J. Vaclavik[1], L. Villard[1]

DRFC, Association Euratom-CEA, CEA Cadarache, 13108 St Paul-lez-Durance, France.
[1] *CRPP, Association Euratom-Confédération Suisse, EPFL, 1015 Lausanne, Switzerland.*
[2] *LPMIA, Université Henri Poincaré-Nancy 1, BP 239, 54506 Vandoeuvre-les-Nancy, France.*

1 Introduction

Understanding and extrapolation of confinement properties remains a key issue for present and future devices. Recent analysis has revealed significant discrepancies between gyrokinetic and fluid calculations. A proper investigation of gyrokinetic turbulence is mandatory to understand turbulent transport in fusion plasmas.
This work deals with non-linear global simulations of instabilities driven by ion temperature gradients (ITG) in an inhomogeneous collisionless plasma confined by a strong uniform magnetic field. Here are presented the first non-linear results obtained with the recently developed Semi-Lagrangian (SL) 4D code.

2 Drift-kinetic model

We consider a collisionless plasma, cylindrical and periodic, which focuses the study to SLAB-ITG modes. The magnetic field is assumed uniform $\vec{B} = B_z\vec{e_z}$ and electrons are considered adiabatics. The Larmor radius effects are neglected so that the ion trajectories are governed by the guiding-center (GC) trajectories, hence :

$$v_{\vec{GC}} = \frac{\vec{E}\times\vec{B}}{B^2} \quad ; \quad \frac{dz}{dt} = v_\parallel \quad ; \quad \dot{v_\parallel} = \frac{q}{m}E_z \tag{1}$$

We assume that there is no fluctuating magnetic field and we use the electrostatic approximation to compute the electric field : $\vec{E} = -\vec{\nabla}\Phi$ where the scalar $\Phi(r,\theta,z,t)$ represents the electric potential. The evolution of the distribution function $f(r,\theta,z,v_\parallel,t)$ is described by the drift-kinetic Vlasov equation :

$$\frac{\partial f}{\partial t} + v_{\vec{GC}}\cdot\vec{\nabla}_\perp f + v_\parallel\frac{\partial f}{\partial z} + \dot{v_\parallel}\frac{\partial f}{\partial v_\parallel} = 0 \qquad \text{with } \vec{\nabla}_\perp = (\frac{\partial .}{\partial r}, \frac{1}{r}\frac{\partial .}{\partial\theta})^t \tag{2}$$

which couples the $\vec{E}\times\vec{B}$ motion across the magnetic field to the motion parallel to the magnetic field. This equation is non-linearly coupled to the quasi-neutrality equation :

$$-\nabla_\perp\cdot\left[\frac{n_0(r)}{B\Omega_0}\nabla_\perp\Phi\right] + \frac{e\,n_0(r)}{T_e(r)}\left(\Phi - \lambda\langle\Phi\rangle\right) = n_i - n_0 \tag{3}$$

where Ω_0 denotes the ion cyclotron frequency ; T_e and n_0 respectively the electron temperature and density profiles. The ion density profile is given by $n_i(r,\theta,z,t) = \int dv_\parallel\, f(r,\theta,z,v_\parallel,t)$ and $\langle\cdot\rangle$ represents the average on the magnetic field lines. The parameter λ is equal to 1 or 0 if the zonal flows are taken into account or not.

3 Linearised dispersion relation

The linearisation of the Vlasov equation (2) and the quasi-neutrality equation (3) is done by splitting f into its Maxwellian equilibrium part and a fluctuating part of first order in the fluctuations. The linear dispersion relation is then :

$$D(\omega) = \left(\kappa(r) + \frac{m^2}{r^2} + \frac{1}{Z_i T_e(r)}\right) T_i(r) + 1 - zZ(z)\{-1 + \frac{\omega^*_{ni}}{\omega} + \frac{\omega^*_{Ti}}{\omega}\left[-\frac{1}{2} + \frac{z}{Z(z)} + z^2\right]\}$$

where Z is the Fried and Conte relation with $z = \frac{\omega}{k_\parallel \sqrt{2T_i}}$ while the diamagnetic drift frequencies are defined by $\omega^*_{Ti} = T_i(r)\frac{d\log T_i(r)}{dr}k_\theta$ and $\omega^*_{ni} = \frac{1}{\eta}\omega^*_{Ti}$ with $\eta = \frac{d\log T_i(r)}{d\log n_0(r)}$. $k_\theta = m/r$ and $k_\parallel = 2\pi n/L_z$ represent the Fourier space vectors, with Lz the cylinder length. The radial electric potential is approximated by $\exp(-g(r))$ where $g(r)$ is chosen such that $\Phi(r)$ is close to the η initial profile. In this case, the function $\kappa(r)$ is

$$\kappa(r) = -\left[\frac{\partial^2 g(r)}{\partial r^2} + \left(\frac{\partial g(r)}{\partial r}\right)^2 + \left(\frac{1}{r} + \frac{1}{n_0(r)}\frac{dn_0(r)}{dr}\right)\frac{\partial g(r)}{\partial r}\right].$$

The solutions $\omega/D(\omega) = 0$ are computed using a Nyquist algorithm, with $\omega = \omega_r + i\gamma$ where ω_r correspond to the frequency and γ to the linear growth rate. The dependence of γ according to the mode numbers m and n is shown in figure 1.

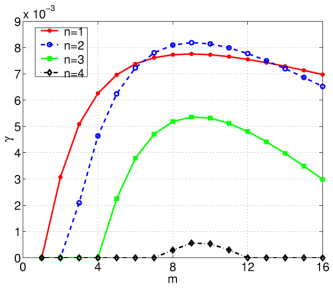

Figure 1: linear growth rate

4 The global Semi-Langrangian code

The non-linear simulations are performed with a recently developed 4D code written in fortran 90 and parallelized with MPI. This code is based on the Semi-Lagrangian method [1]. The purpose of the SL method is to make the best use of the Lagrangian (Particle in Cell code for example) and Eulerian numerical schemes. Therefore to have a good description of the phase space in particular in regions of low density, with an enhanced stability. In this approach, the mesh grid is kept fixed in time in the phase space (Eulerian method) and the Vlasov-equation is integrated along the trajectories (Lagrangian code) using the fact that the distribution function is constant on the trajectories. Cubic spline interpolations are performed to evaluate the new value of the distribution function on the grid points. Indeed, if f is known over the whole fixed grid at the time t, then f at the next time $t + \Delta t$ can be deduced, for each node X_i of the mesh, by $f\left(X_i(t+\Delta t), t+\Delta t\right) = f\left(X(t, X_i, t+\Delta t), t\right)$, where $X(t, X_i, t+\Delta t)$ is the position in the 4D phase space of this point X_i at the previous time t.
The integration along the trajectories is performed with a time-splitting algorithm, which allows one to divided the resolution of the 4D advection equation into the resolution of a succession of 2D and 1D advections. The second order of the global numerical scheme is obtained by conserving a symmetry in the advection and by using a predictor-corrector algorithm in time.

5 Results

The plasma is initialized by exciting a superposition of ITG mode (m, n) with random phase α_{mn} and amplitude ϵ_{mn} such that
$f(r, \theta, z, v_\parallel, 0) = f_M(r, v_\parallel) \times (1 + \sum_{mn} \epsilon_{mn} \cos(\frac{2\pi n}{L_z} z + m\theta + \alpha_{mn}))$ where the Maxwellian

function f_M is defined by $f_M(r, v_\parallel) = (n_0/\sqrt{2\pi T_i/m_i})\exp(-m_i v_\parallel^2/2T_i)$. In the following, the temperature is normalized to T_{e0}, where T_{e0} is defined such that $T_e(r_0)/T_{e0} = 1$ (with r_0 a reference point). The time is normalized to Ω_0^{-1}, the velocity to the sonic velocity $c_s = \sqrt{\frac{T_{e0}}{m_i}}$ and the electric potential to $\frac{T_{e0}}{q_i}$. We impose a vanishing fluctuating part of the distribution function at the boundaries in the r and $v_\parallel$ directions. Periodic boundary conditions are used in the θ and z directions. The electron temperature is kept constant while the ion temperature (fig 2.a) and the density profiles (fig 2.b) are chosen such that the $\eta_i = d\log T_i/d\log n_0$ is larger than 2 in a sufficiently large region to generate instabilities (fig 2.c).

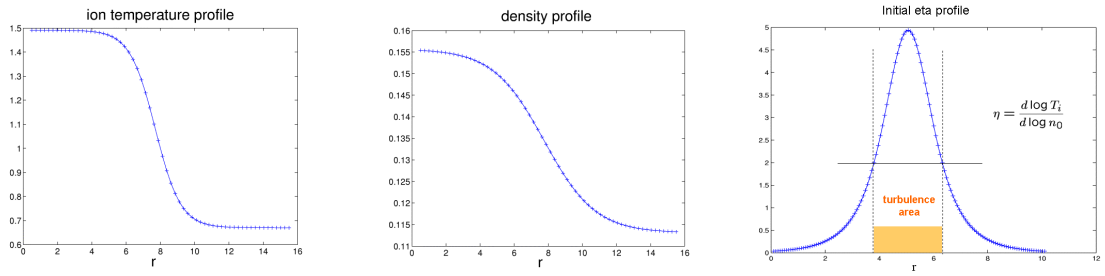

(a) (b) (c)

Figure 2: (a) Ion temperature profile : $T_i(r)$. (b) Density profile : $n_0(r)$. (c) η_i profile.

Role of the zonal flows in the non-linear phase

The SL code is able to simulate the linear and non-linear phase of the SLAB-ITG turbulence. Indeed, we observe an exponential increase in the linear phase (fig. 3), where the linear growth-rate is comparable to the one predicted by the linear study (fig. 1) and the non-linear saturation is well described too. As first non-linear results we present the effect of the zonal flow (case $\lambda = 1$ in (3)) on the turbulent transport. A cross-section of the electric potential shows larger poloidal convection cells in the case $\lambda = 0$. In figures 5.(a) and (b), we see the relaxation of the initial density and ion temperature profiles to the critical threshold values. Besides, comparing the ion temperature profile variation and the flux time evolution, we see the stabilizing effect of the zonal flows.

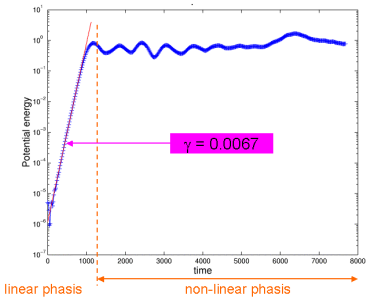

Figure 3: Evolution of Φ^2 : linear phase + non-linear phase

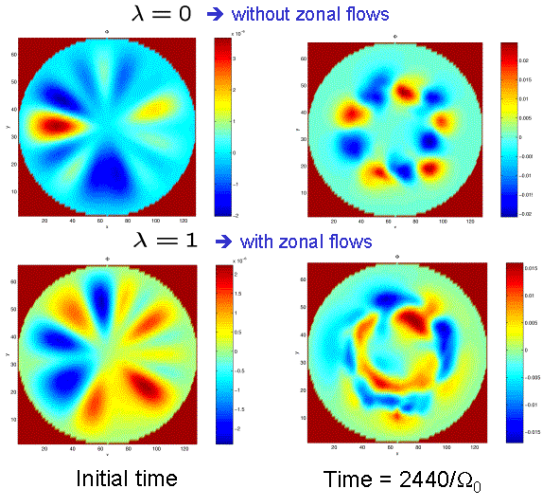

Figure 4: Cross-section of the electric potential in (r, θ), at initial time and time in the saturation phase (t=2440/Ω_0), for both cases $\lambda = 0$ and $\lambda = 1$.

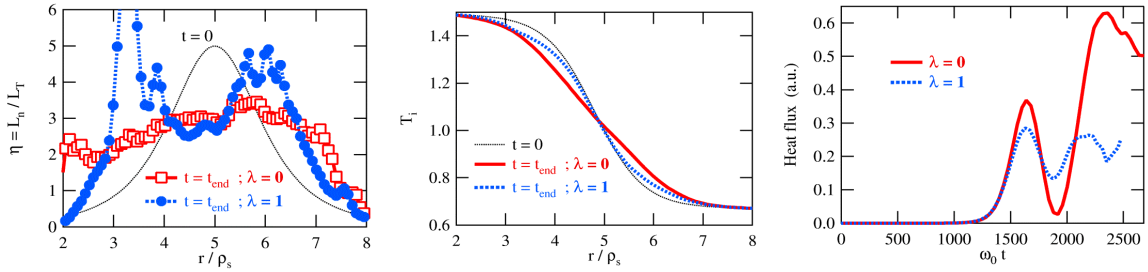

(a) (b) (c)

Figure 5: Comparison without ($\lambda = 0$) and with ($\lambda = 1$) zonal flows for : (a) η profile, (b) ion temperature profile, (c) flux. In (a) and (b) the black lines correspond to the initial state.

Energy and particle conservation

A drawback of the SL method is that the particle conservation is not assured. In our case the number of electrons is constant due to their adiabaticity, but not the number of ions. Nonetheless, the relative error is of the order of 10^{-5} (fig 6.(a)), which is acceptable considering that the order of the interpolation error with cubic splines is of 10^{-6}.In figure 6.(b)), we see that the variation of the kinetic energy $E_{kin} = 1/2 \int (f - f_M) v_\parallel^2 dV\, dv_\parallel$ is balanced by the variation of the potential energy $E_{pot} = 1/2 \int (n_i - n_0) \Phi dV$. However, the total energy $E_{tot} = E_{kin} + E_{pot}$ is not exactly conserved. We still have to understand how this energy conservation can be improved.

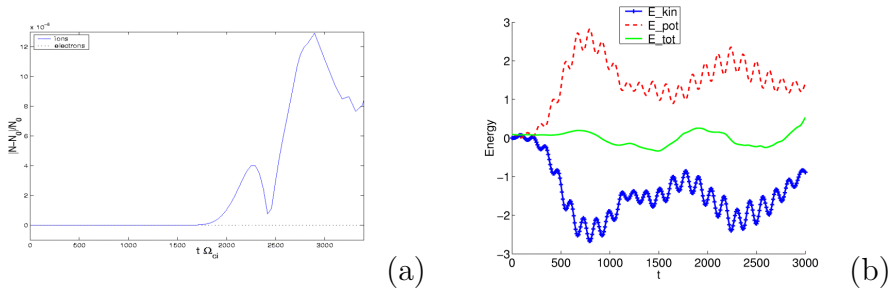

(a) (b)

Figure 6: (a) Relative error of the particle number . (b) Conservation of the total energy

6 Conclusion

A Semi-Lagrangian 4D code has been developed which is able to describe the non-linear phase of the SLAB-ITG turbulence. As first results we have shown the stabilizing effect of the zonal flows. Further investigations are necessary to improve the conservation of the total energy.

References

[1] Sonnendrücker E. et al., 1999 *Journal of Comput. Phys.*, **149**, 201-220.

[2] T.M. Tran et al., 1999 *Proc. Varenna-Lausanne Int. Workshop*, ISPP-18.

[3] Manfredi G et al., 1996 *Phys. Plasmas*, **3** 202.

[4] Depret G. et al., 2000 *Plasma Phys.*, **42** 949.